

Agnostic G^1 Gregory Surfaces

Gerald Farin*
Computer Science
Arizona State University

Dianne Hansford†
FarinHansford.com

April 2, 2012

Abstract

We discuss G^1 smoothness conditions for rectangular and triangular Gregory patches. We then incorporate these G^1 conditions into a surface fitting algorithm. Knowledge of the patch type is inconsequential to the formulation of the G^1 conditions, hence the term *agnostic G^1 Gregory surfaces*.

Keywords: surface fitting, Gregory surfaces, G^1 smoothness conditions, rectangular and triangular patches, point-normal interpolation, tangent ribbon

INSPEC Codes: A,N,P

1 Introduction

Surfaces are used for many modeling purposes, ranging from car bodies or airplane fuselages to objects in animated movies or interactive games. Depending on the application at hand, different surface types are used, such as spline surfaces (Farin [1]) for the first two examples and subdivision surfaces (Peters and Reif [2]) for the last two.

Spline surfaces cover a model with rectangular patches, which can create problems in areas where triangular shapes are needed. Subdivision surfaces have potential problems because direct evaluation is possibly slow (Stam [3]). For this reason, several authors have studied polynomial or rational polynomial approximation subdivision surfaces (Peters [4], Loop et al. [5, 6]).

*Corresponding author: farin@asu.edu, Tempe, AZ 85287-8809, Tel: 480-965-3190, Fax: 480-965-2725

†dianne@farinhansford.com

In this paper, we investigate spline-like surfaces which cover a model by a mix of triangular and rectangular patches. These are rational polynomial patches, first investigated by J. Gregory [7] in rectangular form and by Walton and Meek [8] in triangular form. Our surfaces are G^1 , meaning they have continuous tangent planes everywhere. This is in contrast to spline surfaces, which are typically second order differentiable, or C^2 .

First we introduce rectangular and triangular Gregory surfaces. Next we introduce our G^1 conditions. We then incorporate these G^1 conditions into a surface fitting algorithm.

2 Rectangular Gregory Surfaces

A bicubic Bézier patch is given by a control net

$$\begin{array}{cccc} \mathbf{b}_{00} & \mathbf{b}_{01} & \mathbf{b}_{02} & \mathbf{b}_{03} \\ \mathbf{b}_{10} & \mathbf{b}_{11} & \mathbf{b}_{12} & \mathbf{b}_{13} \\ \mathbf{b}_{20} & \mathbf{b}_{21} & \mathbf{b}_{22} & \mathbf{b}_{23} \\ \mathbf{b}_{30} & \mathbf{b}_{31} & \mathbf{b}_{32} & \mathbf{b}_{33} \end{array}$$

and, for a point $\mathbf{b}(u, v)$ on the patch:

$$\mathbf{b}(u, v) = \sum_{i=0}^3 \sum_{j=0}^3 \mathbf{b}_{ij} \frac{36}{i!j!(3-i)!(3-j)!} (1-u)^{3-i} u^i (1-v)^{3-j} v^j,$$

where the parametric domain is given by $0 \leq u, v \leq 1$. The 3D points \mathbf{b}_{ij} form a control net which determines the shape of the patch.

A “bicubic”¹ Gregory patch (Chiyokura and Kimura [9]) is given by a control net of the same structure but with variable interior control points

$$\begin{aligned} \mathbf{b}_{11} &= \frac{u}{u+v} \mathbf{b}_{11}^{10} + \frac{v}{u+v} \mathbf{b}_{11}^{01}, \\ \mathbf{b}_{21} &= \frac{1-u}{1-u+v} \mathbf{b}_{21}^{10} + \frac{v}{1-u+v} \mathbf{b}_{21}^{01}, \\ \mathbf{b}_{12} &= \frac{u}{1-v+u} \mathbf{b}_{12}^{10} + \frac{1-v}{1-v+u} \mathbf{b}_{12}^{01}, \\ \mathbf{b}_{22} &= \frac{1-u}{2-u-v} \mathbf{b}_{22}^{10} + \frac{1-v}{2-u-v} \mathbf{b}_{22}^{01}. \end{aligned}$$

The superscript 10 identifies Gregory control points with greater influence on the boundaries where u varies, and likewise, the superscript 01 identifies Gregory points

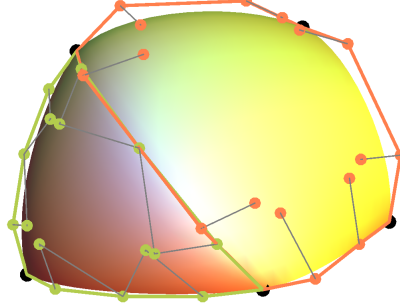


Figure 1: Orange control points: A bicubic rectangular Gregory patch. Green control points: a quartic triangular Gregory patch. Control points are connected to the boundaries to which they yield more influence.

with more influence on the boundaries where v varies. Figure 1 illustrates a bicubic Gregory patch.

The eight interior control points might come from cross boundary continuity conditions. In that context, we will be interested in the degree 3×1 surface formed by the two rows of control points along each edge, called the *tangent ribbon*. Thus the tangent ribbon defines the tangent plane along the boundary. The ribbons along $v = 0$ and $v = 1$ are given by control points

$$\begin{array}{cc} \mathbf{b}_{00} & \mathbf{b}_{01} \\ \mathbf{b}_{10} & \mathbf{b}_{11}^{10} \\ \mathbf{b}_{20} & \mathbf{b}_{21}^{10} \\ \mathbf{b}_{30} & \mathbf{b}_{31} \end{array} \quad \text{and} \quad \begin{array}{cc} \mathbf{b}_{02} & \mathbf{b}_{03} \\ \mathbf{b}_{12}^{10} & \mathbf{b}_{13} \\ \mathbf{b}_{22}^{10} & \mathbf{b}_{23} \\ \mathbf{b}_{32} & \mathbf{b}_{33}, \end{array}$$

respectively. The ribbons along $u = 0$ and $u = 1$ are given by control points

$$\begin{array}{cccc} \mathbf{b}_{00} & \mathbf{b}_{01} & \mathbf{b}_{02} & \mathbf{b}_{03} \\ \mathbf{b}_{10} & \mathbf{b}_{11}^{01} & \mathbf{b}_{12}^{01} & \mathbf{b}_{13} \end{array} \quad \text{and} \quad \begin{array}{cccc} \mathbf{b}_{20} & \mathbf{b}_{21}^{01} & \mathbf{b}_{22}^{01} & \mathbf{b}_{23} \\ \mathbf{b}_{30} & \mathbf{b}_{31} & \mathbf{b}_{32} & \mathbf{b}_{33} \end{array}$$

respectively. Figure 2 (left) illustrates a tangent ribbon for a bicubic Bézier patch.

3 Triangular Gregory Surfaces

A quartic triangular Bézier patch is given by the control net

$$\mathbf{b}_{040}$$

¹The so-called bicubic Gregory patch is rational and degree seven in both u and v .

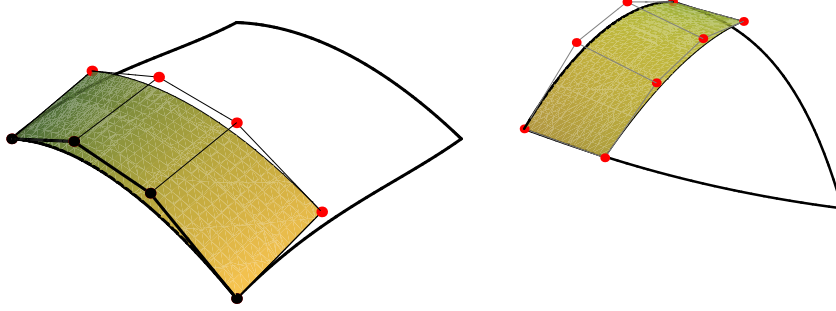


Figure 2: Tangent ribbons for a bicubic rectangular patch (left) and a quartic triangular patch with a cubic boundary curve (right).

$$\begin{array}{ccccccc}
 & & \mathbf{b}_{031} & & \mathbf{b}_{130} & & \\
 & & \mathbf{b}_{022} & \mathbf{b}_{121} & \mathbf{b}_{220} & & \\
 & \mathbf{b}_{013} & \mathbf{b}_{112} & \mathbf{b}_{211} & \mathbf{b}_{310} & & \\
 \mathbf{b}_{004} & \mathbf{b}_{103} & \mathbf{b}_{202} & \mathbf{b}_{301} & \mathbf{b}_{400} & &
 \end{array}$$

and, for a point $\mathbf{b}(u, v, w)$ on the the patch:

$$\mathbf{b}(u, v, w) = \sum_{i+j+k=4} \frac{24}{i!j!k!} u^i v^j w^k \mathbf{b}_{ijk},$$

where the parametric domain is given by barycentric coordinates $u + v + w = 1$.

A triangular Gregory patch (Walton and Meek [8]) is given by a control net of the same structure but with variable interior control points

$$\begin{aligned}
 \mathbf{b}_{112} &= \frac{u}{u+v} \mathbf{b}_{112}^{101} + \frac{v}{u+v} \mathbf{b}_{112}^{011}, \\
 \mathbf{b}_{211} &= \frac{w}{w+v} \mathbf{b}_{211}^{101} + \frac{v}{w+v} \mathbf{b}_{211}^{110}, \\
 \mathbf{b}_{121} &= \frac{u}{u+w} \mathbf{b}_{121}^{110} + \frac{w}{u+w} \mathbf{b}_{121}^{011}.
 \end{aligned}$$

The superscript 101 identifies a Gregory control point with more influence on the $(u, 0, w)$ boundary, the superscript 110 identifies a Gregory point with more influence on the $(u, v, 0)$ boundary, and the superscript 011 identifies a Gregory point with more influence on the $(0, v, w)$ boundary. Figure 1 illustrates a quartic triangular Gregory patch.

Here we will use a special quartic patch in which the three quartic boundary curves

are degree elevated cubics. (This point will be revisited in Sections 4 and 5.) Let the cubic representation of these boundary curves be as follows.

$$\begin{array}{ccccccc} & & & & \mathbf{c}_{030} & & \\ & & & & \mathbf{c}_{021} & \mathbf{c}_{120} & \\ & & & \mathbf{c}_{012} & & \mathbf{c}_{210} & \\ & \mathbf{c}_{003} & \mathbf{c}_{102} & \mathbf{c}_{201} & \mathbf{c}_{300} & & \end{array}$$

Now the tangent ribbons are defined as follows. The ribbon along $u = 0$ is given by control points

$$\begin{array}{ccccccc} & & & & & \mathbf{c}_{030} & \mathbf{c}_{120} \\ & & & & & \mathbf{b}_{121}^{011} & \\ & & & & \mathbf{c}_{021} & & \\ & & & \mathbf{c}_{012} & \mathbf{b}_{112}^{011} & & \\ & \mathbf{c}_{003} & \mathbf{c}_{102} & & & & \end{array}$$

The ribbon along $v = 0$ is given by control points

$$\begin{array}{ccccccc} & & \mathbf{c}_{012} & \mathbf{b}_{112}^{101} & \mathbf{b}_{211}^{101} & \mathbf{c}_{210} & \\ & \mathbf{c}_{003} & \mathbf{c}_{102} & \mathbf{c}_{201} & \mathbf{c}_{300} & & \end{array}$$

The ribbon along $w = 0$ is given by control points

$$\begin{array}{ccccccc} & & \mathbf{c}_{021} & \mathbf{c}_{030} & & & \\ & & \mathbf{b}_{121}^{110} & & \mathbf{c}_{210} & & \\ & & & & \mathbf{b}_{211}^{110} & \mathbf{c}_{120} & \\ & & & & & \mathbf{c}_{201} & \mathbf{c}_{300}. \end{array}$$

Figure 2 (right) illustrates a tangent ribbon for such a Bézier triangle.

The main observation in this paper is that *the above triangular and rectangular G^1 Gregory ribbons have exactly the same structure.* As a consequence, they can be utilized for G^1 surface constructions without a need to know what kind of patch one is dealing with – hence the term “agnostic.”

4 G^1 Conditions

When different surface patches (such as bicubic Bézier ones) are joined together, this is mostly achieved by making them differentiable, or C^1 . Sometimes this is not feasible, and one settles for tangent plane continuity, or G^1 . For an outline of these different concepts, see (Farin [1]).

We give a brief outline of a set of G^1 conditions for two bicubic Bézier patches. Let the two patches have a common boundary curve $\mathbf{q}(t)$ with control polygon $\mathbf{q}_0, \mathbf{q}_1, \mathbf{q}_2, \mathbf{q}_3$. Let patch 1 have an adjacent row of control points $\mathbf{p}_0, \mathbf{p}_1, \mathbf{p}_2, \mathbf{p}_3$. For patch 2, we assume a row $\mathbf{r}_0, \mathbf{r}_1, \mathbf{r}_2, \mathbf{r}_3$. Schematically:

$$\begin{array}{lll}
\mathbf{p}_0 & \mathbf{q}_0 & \mathbf{r}_0 \\
\mathbf{p}_1 & \mathbf{q}_1 & \mathbf{r}_1 \\
\mathbf{p}_2 & \mathbf{q}_2 & \mathbf{r}_2 \\
\mathbf{p}_3 & \mathbf{q}_3 & \mathbf{r}_3
\end{array} \tag{1}$$

For patch 1, all tangent plane information may be obtained from the tangent ribbon formed by the \mathbf{p}_i and \mathbf{q}_i . For patch 2, the tangent ribbon is given by the \mathbf{q}_i and \mathbf{r}_i . In order for the two patches to share a common tangent plane at \mathbf{q}_0 , there must be numbers λ_0, μ_0 such that

$$(1 - \lambda_0)\mathbf{p}_0 + \lambda_0\mathbf{r}_0 = (1 - \mu_0)\mathbf{q}_0 + \mu_0\mathbf{q}_1. \tag{2}$$

Similarly, a common tangent plane at \mathbf{q}_3 necessitates the existence of numbers λ_1, μ_1 such that

$$(1 - \lambda_1)\mathbf{p}_3 + \lambda_1\mathbf{r}_3 = (1 - \mu_1)\mathbf{q}_2 + \mu_1\mathbf{q}_3. \tag{3}$$

Then, $\mathbf{p}_0, \mathbf{q}_1, \mathbf{r}_0, \mathbf{q}_0$ form the tangent plane at \mathbf{q}_0 , and $\mathbf{p}_3, \mathbf{q}_3, \mathbf{r}_3, \mathbf{q}_2$ form the tangent plane at \mathbf{q}_3 .

Conditions for G^1 continuity have been developed (Farin [1]) which require that the tangent ribbons satisfy linear functions $\lambda(t) = (1 - t)\lambda_0 + t\lambda_1$ and $\mu(t) = (1 - t)\mu_0 + t\mu_1$. Express the common boundary as a quartic $\hat{\mathbf{q}}(t)$, obtained from degree elevating the cubic $\mathbf{q}(t)$. Let

$$\mathbf{p}(t) = \sum_{i=0}^3 \mathbf{p}_i B_i^3(t) \quad \mathbf{q}^b(t) = \sum_{i=0}^3 \hat{\mathbf{q}}_i B_i^3(t) \quad \mathbf{q}^a(t) = \sum_{i=1}^4 \hat{\mathbf{q}}_i B_i^3(t) \quad \mathbf{r}(t) = \sum_{i=0}^3 \mathbf{r}_i B_i^3(t),$$

then G^1 continuity is achieved if

$$(1 - \lambda(t))\mathbf{p}(t) + \lambda(t)\mathbf{r}(t) = (1 - \mu(t))\mathbf{q}^b(t) + \mu(t)\mathbf{q}^a(t).$$

Some elementary algebra now leads to a set of G^1 conditions between the two patches:

$$\begin{bmatrix} -3(1 - \lambda_0) & -3\lambda_0 & 0 & 0 \\ (1 - \lambda_1) & \lambda_1 & (1 - \lambda_0) & \lambda_0 \\ 0 & 0 & -3(1 - \lambda_1) & -3\lambda_1 \end{bmatrix} \begin{bmatrix} \mathbf{p}_1 \\ \mathbf{r}_1 \\ \mathbf{p}_2 \\ \mathbf{r}_2 \end{bmatrix} = \begin{bmatrix} ((1 - \lambda_1)\mathbf{p}_0 + \lambda_1\mathbf{r}_0) - ((1 - \mu_1)\hat{\mathbf{q}}_0 + \mu_1\hat{\mathbf{q}}_1) - 3((1 - \mu_0)\hat{\mathbf{q}}_1 + \mu_0\hat{\mathbf{q}}_2) \\ ((1 - \mu_1)\hat{\mathbf{q}}_1 + \mu_1\hat{\mathbf{q}}_2) + ((1 - \mu_0)\hat{\mathbf{q}}_2 + \mu_0\hat{\mathbf{q}}_3) \\ ((1 - \lambda_0)\mathbf{p}_3 - \lambda_0\mathbf{r}_3) - 3((1 - \mu_1)\hat{\mathbf{q}}_2 + \mu_1\hat{\mathbf{q}}_3) - ((1 - \mu_0)\hat{\mathbf{q}}_3 + \mu_0\hat{\mathbf{q}}_4) \end{bmatrix}. \tag{4}$$

Despite the simplicity of these conditions, they have not received much attention in the literature. An exception is work by Tong and Kim [10]. What is somewhat

surprising in our context is the fact that the above G^1 conditions were developed for polynomial patches but they work equally well for rational Gregory patches.

G^1 conditions which use more general functions than the linear ones above are conceivable; for this work, we did not pursue that added generality.

5 G^1 Surface Fitting

Suppose we are given data: a point set with associated normal vectors and a connectivity grouping them into triangular and quadrilateral faces. See Figure 3 for two illustrations. Our goal is to create a triangular or rectangular Gregory patch over each face such that the overall surface is G^1 . The rectangular patches will be bicubic Gregory patches and the triangular patches will be quartic Gregory patches with degree elevated cubics as boundary curves.

We proceed as follows.

1. Build patch boundaries as cubic Bézier curves. We use Piper's point-normal interpolation method [11] which is also used by Vlachos et al. [12] in the context of so-called PN patches. Let \mathbf{p}_i and \mathbf{p}_j be two connected data points with associated normals \mathbf{n}_i and \mathbf{n}_j . We desire a cubic Bézier curve connecting \mathbf{p}_i and \mathbf{p}_j , being perpendicular to \mathbf{n}_i at \mathbf{p}_i and to \mathbf{n}_j at \mathbf{p}_j . We form auxiliary points $\mathbf{c}_i = (2\mathbf{p}_i + \mathbf{p}_j)/3$ and $\mathbf{c}_j = (\mathbf{p}_i + 2\mathbf{p}_j)/3$. Our final Bézier points are

$$\begin{aligned} \mathbf{b}_0 &= \mathbf{p}_i, \\ \mathbf{b}_1 &= \text{projection of } \mathbf{c}_i \text{ onto plane } [\mathbf{p}_i, \mathbf{n}_i], \\ \mathbf{b}_2 &= \text{projection of } \mathbf{c}_j \text{ onto plane } [\mathbf{p}_j, \mathbf{n}_j], \\ \mathbf{b}_3 &= \mathbf{p}_j. \end{aligned}$$

2. Estimate tangent ribbons along the boundary curves. Let us refer to the schematic of (1). Suppose we wish to estimate a ribbon for patch 1, meaning we are given $\mathbf{q}_0, \mathbf{q}_1, \mathbf{q}_2, \mathbf{q}_3$ as well as $\mathbf{p}_0, \mathbf{p}_3$. We need to find estimates for \mathbf{p}_2 and \mathbf{p}_3 , namely \mathbf{p}_2^e and \mathbf{p}_3^e . If patch 1 is a triangular patch, it will be quartic, and we must adjust the tangent ribbon length at the boundary curve ends, namely define

$$\tilde{\mathbf{p}}_0 = (\mathbf{q}_0 + 3\mathbf{p}_0)/4 \quad \text{and} \quad \tilde{\mathbf{p}}_3 = (\mathbf{q}_3 + 3\mathbf{p}_3)/4.$$

To unify the following presentation, if the patch is rectangular let $\tilde{\mathbf{p}}_0 = \mathbf{p}_0$ and $\tilde{\mathbf{p}}_3 = \mathbf{p}_3$. Then the estimates are defined as

$$\begin{aligned} \mathbf{p}_1^e &= \mathbf{q}_1 + 2(\tilde{\mathbf{p}}_0 - \mathbf{q}_0)/3 + (\tilde{\mathbf{p}}_3 - \mathbf{q}_3)/3, \\ \mathbf{p}_2^e &= \mathbf{q}_2 + (\tilde{\mathbf{p}}_0 - \mathbf{q}_0)/3 + 2(\tilde{\mathbf{p}}_3 - \mathbf{q}_3)/3, \end{aligned}$$

Estimates, \mathbf{r}_1^e and \mathbf{r}_2^e , for patch 2 follow similarly.

3. Determine geometry parameters. At $\hat{\mathbf{q}}_0$ there must exist numbers λ_0 and μ_0 such that (2) is met. Since by construction the four points $\tilde{\mathbf{p}}_0, \hat{\mathbf{q}}_0, \tilde{\mathbf{r}}_0, \hat{\mathbf{q}}_1$ are coplanar, this amounts to solving an overdetermined linear system which has an exact solution. We repeat by using $\tilde{\mathbf{p}}_3, \hat{\mathbf{q}}_3, \tilde{\mathbf{r}}_3, \hat{\mathbf{q}}_2$ and (3) for finding λ_1 and μ_1 .

4. Enforce G^1 continuity across interior boundary curves. The two tangent ribbons from step 2 will not ensure G^1 continuity between patch 1 and patch 2. But we can adjust $\mathbf{p}_1, \mathbf{p}_2$ and $\mathbf{r}_1, \mathbf{r}_2$ such that this is the case. Consider the underdetermined linear system $A\mathbf{x} = \mathbf{u}$ in (4) for the four unknowns $\mathbf{p}_1, \mathbf{p}_2, \mathbf{r}_1, \mathbf{r}_2$. (The points $\mathbf{p}_0, \mathbf{p}_3, \mathbf{r}_0, \mathbf{r}_3$ must be replaced by $\tilde{\mathbf{p}}_0, \tilde{\mathbf{p}}_3, \tilde{\mathbf{r}}_0, \tilde{\mathbf{r}}_3$, respectively.) We do have an initial guess

$$\mathbf{x}^e = [\mathbf{p}_1^e, \mathbf{r}_1^e, \mathbf{p}_2^e, \mathbf{r}_2^e]^T$$

for the unknowns from our ribbon estimation, and a solution to (4) is readily found by using an auxiliary linear system

$$AA^T\mathbf{d} = \mathbf{u} - A\mathbf{x}^e, \quad (5)$$

then the final solution is given by

$$\mathbf{x} = \mathbf{x}^e + A^T\mathbf{d}. \quad (6)$$

Note that A has full row rank since $\hat{\mathbf{q}}$ is truly a cubic.² This approach to solving an underdetermined linear system is taken from Boehm and Prautzsch [13]. The explicit solution may be expressed using the matrix $A^T(AA^T)^{-1}$, which is the Moore-Penrose pseudoinverse to (4), thus explaining why we in fact minimize the distance to our initial guess \mathbf{x}^e .³

We use least squares to solve (5) for reasons of numerical stability.

5. Load Gregory patches with tangent ribbon data. Points $\mathbf{p}_1, \mathbf{p}_2, \mathbf{r}_1, \mathbf{r}_2$ must be stored in the appropriate Gregory point position. In addition, the common boundary control polygons must be recorded, which is \mathbf{q} for a rectangular patch and $\hat{\mathbf{q}}$ for a triangular patch. If a boundary has no neighbor, then simply load the boundary curve and guess interior points computed in steps 1 and 2.

6 Examples

We demonstrate our G^1 construction using two examples. Example 1 is a symmetric data set; Example 2 exhibits very little symmetry.

Figure 3 shows the input data: data points, given normals, and data connectivity.

The boundary curves are shown in Figure 4. They are generated according to step 1 above.

²Tae-wan Kim, private communication 2011

³A reviewer kindly pointed this out to us.

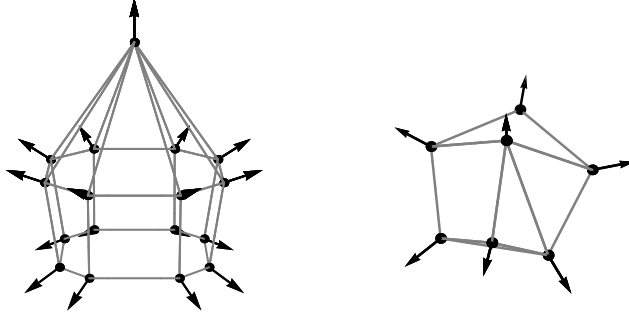


Figure 3: Input data. Left: Example 1, right: Example 2.

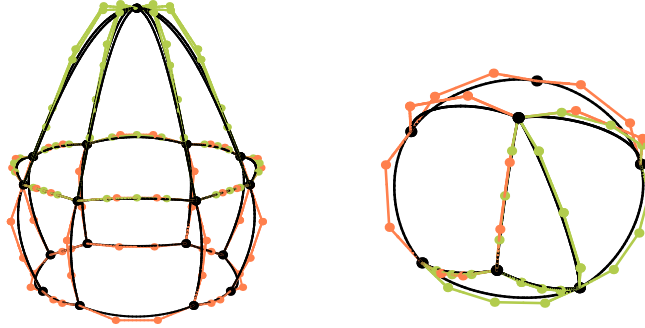


Figure 4: Patch boundary curves. Left: Example 1, right: Example 2.

The initial guesses for the control nets are shown in Figure 5. This follows step 2 above. Note that the resulting surface is only G^0 .

The results of the G^1 construction of steps 3 and 4 are shown in Figure 6. All creases which resulted from step 2 are now eliminated. The Example 2 surface still has some shape defects that were introduced by the initial guess, however, it is G^1 .

7 Conclusion

We presented a framework for the construction of G^1 Gregory surfaces. This framework handles rectangular surfaces in the same manner as triangular ones, based on the concept of cubic tangent ribbons.

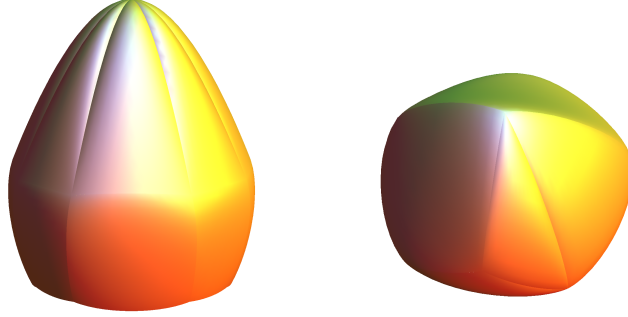


Figure 5: Initial guesses. Left: Example 1, right: Example 2.

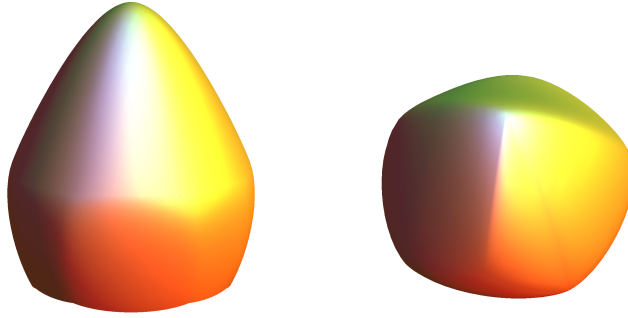


Figure 6: Final G^1 surfaces. Left: Example 1, right: Example 2.

More work is needed, however:

1. Piper's boundary curve generation method is very ad hoc and does not always yield good results. Walton and Meek [8] suggest a more involved method; a combination of ideas from that paper with Piper's might yield more satisfying shapes.
2. Our tangent ribbon estimator may be too simplistic. While any tangent ribbon estimate will ultimately lead to a G^1 surface, its shape does depend on the estimate. In cases such as approximating subdivision surfaces, additional data are available which may be utilized.
3. Our G^1 conditions utilize linear functions $\lambda(t)$ and $\mu(t)$. More research might lead to more suitable (higher degree?) functions.

References

- [1] G. Farin. *Curves and Surfaces for Computer Aided Geometric Design*. Morgan-Kaufmann, 2001. Fifth edition.
- [2] J. Peters and U. Reif. *Subdivision Surfaces*. Springer, 2008.
- [3] J. Stam. Exact evaluation of Catmull-Clark subdivision surfaces at arbitrary parameter values. In *Computer Graphics Proceedings*, pages 395–404, 1998.
- [4] J. Peters. Smooth interpolation of a mesh of curves. *Constructive Approximation*, 7(2):221–247, 1991.
- [5] C. Loop and S. Schaefer. Approximating Catmull-Clark surfaces with bicubic patches. *ACM Transactions on Graphics*, 27(1):1–11, 2008.
- [6] C. Loop, S. Schaefer, T. Ni, and I. Castano. Approximating subdivision surfaces with Gregory patches for hardware tessellation. *ACM Transactions on Graphics*, 28(1):1–9, 2009.
- [7] J. Gregory. Smooth interpolation without twist constraints. In R. E. Barnhill and R. F. Riesenfeld, editors, *Computer Aided Geometric Design*, pages 71–88. Academic Press, 1974.
- [8] D. Walton and D. Meek. A triangular G^1 patch from boundary curves. *Computer Aided Design*, 28(2), 1996.
- [9] H. Chiyokura and F. Kimura. A new surface interpolation method for irregular curve models. *Computer Graphics Forum*, (3):209–218, 1984.
- [10] Wei hua Tong and Tae wan Kim. High-order approximation of implicit surfaces by G^1 triangular spline surfaces. *Computer Aided Design*, 41, 2009.
- [11] B. Piper. Visually smooth interpolation with triangular Bézier patches. In G. Farin, editor, *Geometric Modeling: Algorithms and New Trends*, pages 221–233. SIAM, Philadelphia, 1987.
- [12] A. Vlachos, J. Peters, C. Boyd, and J. Mitchell. Curved PN triangles. In *ACM Symposium on Interactive 3D Graphics 2001*, pages 159–166, 2001.
- [13] W. Boehm and H. Prautzsch. *Numerical Methods*. Vieweg, 1992.